

Precision Matrix Regularization in Sufficient Dimension Reduction for Improved Quadratic Discriminant Classification

Derik T. Boonstra^a, Rakheon Kim^a and Dean M. Young^a

^aDepartment of Statistical Science, Baylor University, Waco, TX 76798-7140

ARTICLE INFO

Keywords:

Central subspace
Covariance sparsity
Heteroscedasticity
Shrinkage estimator
Singular value decomposition

ABSTRACT

Sufficient dimension reduction (SDR) methods, which often rely on class precision matrices, are widely used in supervised statistical classification problems. However, when class-specific sample sizes are small relative to the original feature-space dimension, precision matrix estimation becomes unstable and, as a result, increases the variability of the linear dimension reduction (LDR) matrix. Ultimately, this fact causes suboptimal supervised classification. To address this problem, we develop a multiclass and distribution-free SDR method, stabilized SDR (SSDR), that employs user-specified precision matrix shrinkage estimators to stabilize the LDR projection matrix and supervised classifier. We establish this technique with the theoretical guarantee of preserving all classification information under the quadratic discriminant analysis (QDA) decision rule. We evaluate multiple precision matrix shrinkage estimators within our proposed SSDR framework through Monte Carlo simulations and applications to real datasets. Our empirical results demonstrate the efficacy of the SSDR method, which generally improves classification accuracy and frequently outperforms several well-established competing SDR methods.

1. Introduction

For statistical discriminant analysis and other parametric multivariate statistical methods, one generally must estimate the precision matrix. However, this task becomes challenging when the feature-space dimension, p , is large relative to the class-specific sample size, n_i , $i = 1, \dots, k$, where k is the *a priori* number of classes. With advancements in computing, recent literature has increasingly focused on addressing dimensionality issues in precision matrices and classification in high-dimensional scenarios, $n_i < p$. However, issues may still arise in discriminant analysis for heteroscedastic populations due to precision estimation when $n_i > p$, specifically, when $p < n_i < p^2/2$, which Bellman (1961) first referred to as *the curse of dimensionality*. In general statistical methods and discriminant analysis, we can avoid the *curse of dimensionality* by using *SDR* to reduce the feature-space dimension to a lower dimension, $q < p$.

Anderson (1951) developed *QDA* as a generalization of Fisher (1936)'s *linear discriminant analysis (LDA)* to incorporate differences in covariance matrices. However, Gaynanova et al. (2016) found that *QDA* may suffer from the *curse of dimensionality* and perform poorly in terms of the *conditional error rate (CER)* if an insufficient sample size is used to estimate the $(k-1)+kp+kp(p+1)/2$ parameters required under heteroscedasticity. As a result, they concluded that even when covariance matrices differ, *QDA* can perform worse than *LDA* in terms of the *CER* when training-sample sizes are small. This result occurs because pooling covariance matrices in *LDA* substantially reduces the total number of parameters to estimate. Alternatively, by projecting the data onto a lower dimensional and information preserving subspace, *SDR* techniques reduce the number of free parameters and allow for the additional benefit of preserving heteroscedastic classification information under the *QDA* decision rule. More specifically, let $Y \in \mathbb{R}$ be the univariate response of $\mathbf{X} \in \mathbb{R}^p$. Then, *SDR* techniques aim to identify the smallest possible reduced data dimension $q < p$ such that $\mathbf{R}(\mathbf{X}) \in \mathbb{R}^q$ where no loss of information occurs in $Y|\mathbf{R}(\mathbf{X})$ with respect to $Y|\mathbf{X}$.

In *SDR*, the dimension reduction is usually constrained to be a linear transformation such that $\mathbf{R}(\mathbf{X}) = \mathbf{B}^T \mathbf{X}$, $\mathbf{B} \in \mathbb{R}^{p \times q}$. Thus, we say the dimension reduction is a *sufficient linear reduction* if it satisfies at least one of the following: (i) $Y \perp\!\!\!\perp \mathbf{X}|\mathbf{B}^T \mathbf{X}$, (ii) $\mathbf{X}|(Y, \mathbf{B}^T \mathbf{X}) \sim \mathbf{X}| \mathbf{B}^T \mathbf{X}$, or (iii) $Y|\mathbf{X} \sim Y|\mathbf{B}^T \mathbf{X}$. The subspace \mathcal{S} , defined by $\text{span}(\mathbf{B}) \subseteq \mathbb{R}^p$, is then called a *dimension reduction subspace (DRS)*. Moreover, \mathcal{S} is said to be a *minimum DRS* for $Y|\mathbf{X}$ if $\dim(\mathcal{S}) \leq \dim(\mathcal{S}_{DRS})$ for every *DRS*, \mathcal{S}_{DRS} . However, a *minimum DRS* may not be unique. To address this issue, Cook (1998) first introduced the *central subspace (CS)*, defined as the intersection of all dimension reduction subspaces, denoted as $\mathcal{S}_{Y|\mathbf{X}} = \cap \mathcal{S}_{DRS}$. Given that $\cap \mathcal{S}_{DRS}$ itself is a *DRS*, then under mild conditions given by Cook (1998), $\mathcal{S}_{Y|\mathbf{X}}$ exists and is the *unique minimum DRS*, serving as the target subspace for most *SDR* methods. Throughout the paper, we assume the existence of the *CS*.

For supervised classification, most *SDR* methods are used in a two-stage reduce-and-classify approach. That is, we first derive an *LDR* projection matrix to reduce the feature-space dimension and then apply an appropriate supervised classification rule. These *SDR* methods often construct their *LDR* projection matrix with some function of the first two conditional moments for each labeled population. This *SDR* approach includes the popular *Sliced Inverse Regression (SIR)*, proposed by Li (1991), which reduces the dimensionality by estimating subspaces that capture the response variability by slicing the data along different directions. To enhance robustness, Cook and Weisberg (1991) extended *SIR* by incorporating the variability within

each slice through the k conditional covariance matrices. Other *SDR* techniques construct a targeted *DRS* by optimizing differentiable multivariate functions. For example, Zhang and Mai (2019) proposed a envelope discrimination method, which estimates reduced subspaces and uses envelope methods to develop a classification rule within the same model. Alternative *SDR* methods have also been proposed, such as those by Cook and Zhang (2014), Lin et al. (2019), Qian et al. (2019), Wu and Hao (2022), Zeng et al. (2024), and Mai et al. (2025). For a comprehensive review of *SDR*, see Cook (2018) and Li (2018).

Here, we propose and evaluate a new *SDR* technique, *Stabilized SDR (SSDR)*, which utilizes a user-specified precision matrix shrinkage estimator to stabilize the *LDR* matrix when class parameters must be estimated. By preserving the differences among covariance matrices and reducing variability by regularizing the k precision matrices, our proposed *SSDR* method maintains or improves upon the full-feature estimated *CER* in smaller data dimensions under the *QDA* decision rule. Moreover, we have found strong evidence that the estimated *CER* is often significantly reduced in cases when the class-specific training-sample sizes are small relative to the original feature-space dimensionality. Using *Monte Carlo (MC)* simulations and real datasets that vary in training-sample sizes, feature-space dimensions, and number of classes, we contrast the efficacy of four precision matrix shrinkage estimators that can be utilized with this new *SDR* method. For a comprehensive review of other precision matrix estimators, see Fan et al. (2016). Additionally, we demonstrate that our proposed *SSDR* method provides superior classification performance in terms of smaller estimated *CERs* by frequently outperforming competitive *SDR* and supervised classification techniques.

The remainder of the paper proceeds as follows. In Section 2, we establish the notation used throughout the paper and formally define the *QDA* classifier. Next, we derive a theoretical *SDR* method that preserves the optimal error rate under the *QDA* decision rule when all group parameters are known. For the usual case when class parameters must be estimated, we provide a modification that yields improved *LDR* projection matrix stabilization by employing a shrinkage estimator for each class-specific precision matrix. In Section 3, we introduce four precision matrix estimators for possible use in our proposed *SSDR* technique. We next describe our *MC* simulation design for multiple population configurations and present simulation results in Section 4. In Section 5, we describe our application to several real datasets to further assess the utility of our proposed *SSDR* method and then discuss the results. Moreover, we demonstrate that, in most of the real data applications considered, our proposed *SSDR* method outperforms several current competing *SDR* and classification techniques in terms of the estimated *CER*. Lastly, in Section 6, we discuss our new *SDR* methodology and results.

2. Notation, Preliminaries, and an SDR Method

The following notation will be used throughout the remainder of the paper. Let $\mathbb{R}^{m \times n}$ represent the set of all $m \times n$ real matrices. For $i = 1, \dots, k$, let Π_i represent the i^{th} distinct population or class, let π_i be the *a priori* class membership, let $\Sigma_i \in \mathbb{R}^{p \times p}$ denote the i^{th} population covariance matrix, and let $\mu_i \in \mathbb{R}^p$ be the population mean vector for the i^{th} population. Also, let $\mathbb{S}^p \subset \mathbb{R}^{p \times p}$ represent the set of $p \times p$ real symmetric matrices, and let $\mathbb{S}_+^p \subset \mathbb{S}^p$ denote the interior of the cone of $p \times p$ real symmetric positive-definite matrices. For $\mathbf{A} \in \mathbb{R}^{m \times n}$, we let $\mathbf{A}^+ \in \mathbb{R}^{n \times m}$ denote the Moore-Penrose pseudo-inverse, $C(\mathbf{A})$ represent the column space, and $\mathcal{N}(\mathbf{A})$ denote the null space of \mathbf{A} . Lastly, let $\mathbf{A} = \mathbf{U}\mathbf{D}\mathbf{V}^T$ be the *singular value decomposition (SVD)* of Eckart and Young (1936), where $\mathbf{U} \in \mathbb{R}^{m \times m}$ and $\mathbf{V} \in \mathbb{R}^{n \times n}$ are orthonormal matrices, and $\mathbf{D} \in \mathbb{R}^{m \times n}$ is a diagonal matrix of the singular values of \mathbf{A} .

2.1. Quadratic Discriminant Analysis

Suppose one desires to obtain a supervised classification decision rule that partitions the feature-space into k disjoint regions, \mathbb{R}_{Π_i} , $i = 1, \dots, k$, corresponding to each respective population. Then, we assign an unlabeled observation, $\mathbf{x} \in \mathbb{R}^p$, to Π_i if $\mathbf{x} \in \mathbb{R}_{\Pi_i}$. We consider the criterion function for the i^{th} class to be

$$d_i(\mathbf{x}) := \log |\Sigma_i| - 2 \log (\pi_i) + (\mathbf{x} - \mu_i)^T \Sigma_i^{-1} (\mathbf{x} - \mu_i), \quad i = 1, \dots, k. \quad (1)$$

Thus, we obtain the well-established *QDA* decision criterion. That is, *QDA* classifies an unlabeled observation \mathbf{x} into the class Π_i if $d_i(\mathbf{x}) = D(\mathbf{x})$, where

$$D(\mathbf{x}) := \min \{d_i(\mathbf{x}) : i = 1, \dots, k\}. \quad (2)$$

Generally, we must estimate the population parameters μ_i and Σ_i from the training data such that $n_i > p$. Thus, (1) becomes

$$\hat{d}_i(\mathbf{x}) := \log |\mathbf{S}_i| - 2 \log (\pi_i) + (\mathbf{x} - \bar{\mathbf{x}}_i)^T \mathbf{S}_i^{-1} (\mathbf{x} - \bar{\mathbf{x}}_i), \quad i = 1, \dots, k, \quad (3)$$

where $\bar{\mathbf{x}}_i$ and \mathbf{S}_i are the maximum likelihood estimates of μ_i and Σ_i , respectively. For this training-data scenario, the supervised *QDA* decision rule uses (3) rather than $d_i(\mathbf{x})$ in (2).

2.2. An SDR Theorem

We now present a theoretical result that yields an *SDR*-based *LDR* transformation of the full-dimensional feature data that preserves the optimal error rate associated with the full-dimensional feature-space under the *QDA* decision rule when all population mean vectors and covariance matrices are known. This result is motivated by the concept from Peters et al. (1978)

of linear sufficiency for differences in k heteroscedastic multivariate populations. Ounpraseuth et al. (2015) have derived similar results under the multivariate normality assumption. However, our results, presented in the theorem below and the lemmas in the appendix, are distribution-free. Additionally, we make no assumption concerning prior probabilities for classes. We remark that Xie and Qiu (2007) have found that unequal class prior probabilities negatively affect the performance of *QDA* in terms of the *Area Under the Receiver Operating Characteristic Curve (AUC)*. However, Xue and Titterington (2008) have demonstrated that although re-balancing training-sample sizes may lead to a marginal increase in the *AUC*, a relatively large increase in the *CER* often follows.

The *SDR* approach presented in the theorem provides necessary and sufficient conditions such that classification of an unlabeled observation into a population remains invariant when we use the linearly-transformed lower-dimensional data.

Theorem. Suppose we have k multivariate populations with full classification information contained in the population means $\boldsymbol{\mu}_i$ and population covariance matrices $\boldsymbol{\Sigma}_i \in \mathbb{S}_+^p$, where $i = 1, \dots, k$. Let π_i denote a priori class membership, and let

$$\mathbf{M} := [\boldsymbol{\Sigma}_2^{-1} \boldsymbol{\mu}_2 - \boldsymbol{\Sigma}_1^{-1} \boldsymbol{\mu}_1 | \dots | \boldsymbol{\Sigma}_k^{-1} \boldsymbol{\mu}_k - \boldsymbol{\Sigma}_1^{-1} \boldsymbol{\mu}_1 | \boldsymbol{\Sigma}_2 - \boldsymbol{\Sigma}_1 | \dots | \boldsymbol{\Sigma}_k - \boldsymbol{\Sigma}_1], \quad (4)$$

where $\mathbf{M} \in \mathbb{R}^{p \times s}$, $s = (k-1)(p+1)$ with $\text{rank}(\mathbf{M}) = q < p$. Let $\mathbf{M} = \mathbf{UDV}^T \in \mathbb{R}^{p \times s}$ be the reduced SVD of \mathbf{M} , where $\mathbf{U} \in \mathbb{R}^{p \times q}$, $\text{rank}(\mathbf{U}) = q < p$, $\mathbf{D} \in \mathbb{R}^{q \times q}$, and $\mathbf{V} \in \mathbb{R}^{s \times q}$. Then, for an unlabeled observation vector $\mathbf{x} \in \mathbb{R}^p$, $D(\mathbf{x}) = D(\mathbf{U}^T \mathbf{x})$, where $D(\mathbf{x})$ is defined in (2).

Proof. First let $\mathbf{U} \in \mathbb{R}^{p \times q}$ with $\text{rank}(\mathbf{U}) = q$. Now let $\mathbf{P}_U^\perp := (\mathbf{I} - \mathbf{U}\mathbf{U}^T)$ and $\mathbf{C} := \mathbf{R}\mathbf{P}_U^\perp$, where $\mathbf{R} \in \mathbb{R}^{(p-q) \times p}$ and $\text{rank}(\mathbf{R}) = p - q$. Using Lemmas 1, 2, and 3 in the appendix and letting $\mathbf{A} = [\mathbf{U}^T, \mathbf{C}^T]^T \in \mathbb{S}_+^p$, we have that

$$\begin{aligned} d_i(\mathbf{x}) &= d_i(\mathbf{Ax}) \\ &= -2 \log(\pi_i) + \log \left| \mathbf{A} \boldsymbol{\Sigma} \mathbf{A}^T \right| + [\mathbf{A}(\mathbf{x} - \boldsymbol{\mu}_i)]^T (\mathbf{A} \boldsymbol{\Sigma}_i \mathbf{A}^T)^{-1} [\mathbf{A}(\mathbf{x} - \boldsymbol{\mu}_i)] \\ &= -2 \log(\pi_i) + \log \left| \begin{array}{cc} \mathbf{U}^T \boldsymbol{\Sigma}_i \mathbf{U} & \mathbf{U}^T \boldsymbol{\Sigma}_i \mathbf{C}^T \\ \mathbf{C} \boldsymbol{\Sigma}_i \mathbf{U} & \mathbf{C} \boldsymbol{\Sigma}_i \mathbf{C}^T \end{array} \right| \\ &\quad + \left[\begin{array}{c} \mathbf{U}^T(\mathbf{x} - \boldsymbol{\mu}_i) \\ \mathbf{C}(\mathbf{x} - \boldsymbol{\mu}_i) \end{array} \right]^T \left[\begin{array}{cc} \mathbf{U}^T \boldsymbol{\Sigma}_i \mathbf{U} & \mathbf{U}^T \boldsymbol{\Sigma}_i \mathbf{C}^T \\ \mathbf{C} \boldsymbol{\Sigma}_i \mathbf{U} & \mathbf{C} \boldsymbol{\Sigma}_i \mathbf{C}^T \end{array} \right]^{-1} \left[\begin{array}{c} \mathbf{U}^T(\mathbf{x} - \boldsymbol{\mu}_i) \\ \mathbf{C}(\mathbf{x} - \boldsymbol{\mu}_i) \end{array} \right] \\ &= -2 \log(\pi_i) + \log \left| \begin{array}{cc} \mathbf{U}^T \boldsymbol{\Sigma}_i \mathbf{U} & \mathbf{0} \\ \mathbf{0} & \mathbf{C} \boldsymbol{\Sigma}_i \mathbf{C}^T \end{array} \right| \\ &\quad + \left[\begin{array}{c} \mathbf{U}^T(\mathbf{x} - \boldsymbol{\mu}_i) \\ \mathbf{C}(\mathbf{x} - \boldsymbol{\mu}_i) \end{array} \right]^T \left[\begin{array}{cc} \mathbf{U}^T \boldsymbol{\Sigma}_i \mathbf{U} & \mathbf{0} \\ \mathbf{0} & \mathbf{C} \boldsymbol{\Sigma}_i \mathbf{C}^T \end{array} \right]^{-1} \left[\begin{array}{c} \mathbf{U}^T(\mathbf{x} - \boldsymbol{\mu}_i) \\ \mathbf{C}(\mathbf{x} - \boldsymbol{\mu}_i) \end{array} \right] \\ &= -2 \log(\pi_i) + \log \left| \mathbf{U}^T \boldsymbol{\Sigma}_i \mathbf{U} \right| + \log \left| \mathbf{C} \boldsymbol{\Sigma}_i \mathbf{C}^T \right| \\ &\quad + [\mathbf{U}^T(\mathbf{x} - \boldsymbol{\mu}_i)]^T \mathbf{U}^T \boldsymbol{\Sigma}_i^{-1} \mathbf{U} [\mathbf{U}^T(\mathbf{x} - \boldsymbol{\mu}_i)] \\ &\quad + [\mathbf{C}(\mathbf{x} - \boldsymbol{\mu}_i)]^T [\mathbf{C} \boldsymbol{\Sigma}_i \mathbf{C}^T]^{-1} [\mathbf{C}(\mathbf{x} - \boldsymbol{\mu}_i)] \\ &= -2 \log(\pi_i) + \log \left| \mathbf{U}^T \boldsymbol{\Sigma}_i \mathbf{U} \right| + [\mathbf{U}^T(\mathbf{x} - \boldsymbol{\mu}_i)]^T \mathbf{U}^T \boldsymbol{\Sigma}_i^{-1} \mathbf{U} [\mathbf{U}^T(\mathbf{x} - \boldsymbol{\mu}_i)] + c \\ &= d_i(\mathbf{U}^T \mathbf{x}) + c, \end{aligned}$$

where $c := \log \left| \mathbf{C} \boldsymbol{\Sigma}_i \mathbf{C}^T \right| + [\mathbf{C}(\mathbf{x} - \boldsymbol{\mu}_i)]^T [\mathbf{C} \boldsymbol{\Sigma}_i \mathbf{C}^T]^{-1} [\mathbf{C}(\mathbf{x} - \boldsymbol{\mu}_i)]$. Because c is fixed for the reference parameters $\boldsymbol{\mu}_1$ and $\boldsymbol{\Sigma}_1$, we have $d_i(\mathbf{x}) > d_j(\mathbf{x})$ if and only if $d_i(\mathbf{U}^T \mathbf{x}) > d_j(\mathbf{U}^T \mathbf{x})$ for all $i, j = 1, \dots, k; i \neq j$. Therefore, $D(\mathbf{x}) = D(\mathbf{U}^T \mathbf{x})$. The arguments are reversible and, thus, the theorem holds. \square

In the above theorem, assuming all parameters are known, the *DRS* is $\mathcal{S}_M := \text{span}(\mathbf{M})$. Because \mathbf{U}^T provides a basis for $\mathcal{S}_M \subseteq \mathcal{S}_{Y|\mathbf{X}}$, a relationship guaranteed by the linearity condition of $E[\mathbf{X}|\mathbf{U}^T \mathbf{X}]$, we have derived an *SDR* projection matrix that preserves the full-dimensional optimal error rate under the *QDA* decision rule. Thus, we can replace an unlabeled vector $\mathbf{x} \in \mathbb{R}^p$ with the lower-dimensional vector $\mathbf{U}^T \mathbf{x} \in \mathbb{R}^q$, $q < p$, with no loss of supervised classification information.

2.3. An SDR Method with Precision Matrix Shrinkage Estimators

In Section 1, we discuss the benefits of *SDR* methods in terms of efficiency for parameter estimation. Moreover, we seek to improve upon the use of *SDR* in supervised classification by avoiding the over-parametrization that often occurs with a relatively small training-sample size. We can achieve this improvement by reducing the variability of the class-specific precision matrix estimators for $\boldsymbol{\Omega}_i = \boldsymbol{\Sigma}_i^{-1}$. Thus, motivated by the theorem in Section 2.2, we propose a new *SDR* method that adds stability to the *LDR* projection matrix through induced sparsity and bias by utilizing a specified precision shrinkage

estimator. Let $\hat{\Omega}_i$ be an estimator of Ω_i . Then when the parameters are unknown, we replace the columns of \mathbf{M} in (4) with their sample estimates and user-specified precision estimators, yielding

$$\hat{\mathbf{M}} := \left[\hat{\Omega}_2 \bar{\mathbf{x}}_2 - \hat{\Omega}_1 \bar{\mathbf{x}}_1 | \dots | \hat{\Omega}_k \bar{\mathbf{x}}_k - \hat{\Omega}_1 \bar{\mathbf{x}}_1 | \mathbf{S}_2 - \mathbf{S}_1 | \dots | \mathbf{S}_k - \mathbf{S}_1 \right]. \quad (5)$$

In the theorem, we show that multiplying an unlabeled observation $\mathbf{x} \in \mathbb{R}^p$ by the *SDR*-based *LDR* projection matrix $\mathbf{U}^T \in \mathbb{R}^{q \times p}$ preserves all classification information in a reduced q -dimensional subspace. However, we cannot directly obtain \mathbf{U}^T when $\text{rank}(\hat{\mathbf{M}}) = p$. Moreover, we may wish to obtain a lower dimensional representation of the original data with dimension r , where $1 \leq r \leq q < p$. Thus, we look to construct an r -dimensional *SDR*-based *LDR* projection matrix that preserves all of the original p -dimensional classification information. Let $\mathbf{U}_{(r)} \in \mathbb{R}^{p \times r}$ denote the matrix composed of the r vectors of \mathbf{U} corresponding to the r largest singular values in the SVD. Finally, let $\hat{\mathbf{M}} = \mathbf{U}_{\hat{\mathbf{M}}} \mathbf{D}_{\hat{\mathbf{M}}} \mathbf{V}_{\hat{\mathbf{M}}}^T$ be the SVD of (5). Then we define $\mathbf{U}_{\hat{\mathbf{M}},(r)}^T \in \mathbb{R}^{r \times p}$ to be the r -dimensional *SDR*-based *LDR* projection matrix for reducing the feature dimension from dimension p to the smaller dimension r . We refer to this *SDR* method as *stabilized SDR* (*SSDR*).

For supervised classification purposes, we project an unlabeled observation $\mathbf{x} \in \mathbb{R}^p$ by applying the linear transformation $\mathbf{U}_{\hat{\mathbf{M}},(r)}^T \mathbf{x} \in \mathbb{R}^r$ and then applying a specified classification rule to the resulting r -dimensional reduced data. Our *SSDR* approach provides a general *SDR* technique usable with any supervised classification method. However, here, we adopt the supervised *QDA* decision rule in (3) for classification because our *SSDR* method is motivated by the theorem in Section 2.2 and incorporates heteroscedastic information. Lastly, for selecting the optimal dimension r , we propose the estimated *CER* using a cross-validation method as the criterion.

3. Four Precision Matrix Shrinkage Estimators

In this section, we describe four precision matrix shrinkage estimators proposed by Molstad and Rothman (2018), Haff (1979a), Wang et al. (2015), and Bodnar et al. (2016) that we use to formulate our proposed *SSDR* method, described in Section 2.3. We refer to these four precision matrix estimators as the *MRY*, *Haff*, *Wang*, and *Bodnar* estimators, respectively.

3.1. MRY Estimator

The first precision matrix shrinkage estimator we consider was proposed by Molstad and Rothman (2018) and is given by

$$\hat{\Omega}_i := \arg \min_{\Omega_* \in \mathbb{S}_+^p} \{ \text{tr}(\mathbf{S}_i \Omega_*) - \log |\Omega_*| + \lambda_i^* |\mathbf{A}_i \Omega_* \mathbf{B}_i - \mathbf{C}_i|_1 \}, \quad (6)$$

where $\lambda_i^* > 0$ is a tuning parameter, and $\mathbf{A}_i \in \mathbb{R}^{a \times p}$, $\mathbf{B}_i \in \mathbb{R}^{p \times b}$, and $\mathbf{C}_i \in \mathbb{R}^{a \times b}$ are user-specified matrices. Also, $|\mathbf{M}|_1 = \sum_{l \neq j} |\mathbf{M}_{lj}|$ is an L_1 -like norm that forces sparsity on the off-diagonal elements. This shrinkage estimator exploits the assumption that $\mathbf{A}_i \Omega_* \mathbf{B}_i - \mathbf{C}_i$ is sparse and uses \mathbf{C}_i as a shrinkage target matrix for $\mathbf{A}_i \Omega_* \mathbf{B}_i - \mathbf{C}_i$.

For *QDA*, Molstad and Rothman (2018) have proposed the specified matrices $\mathbf{C}_i = \mathbf{0}_p$, a $p \times p$ matrix of zeros, and $\mathbf{A}_i^T = \mathbf{B}_i = (\bar{\mathbf{x}}_i, \gamma_i \mathbf{I}_p)$ for the tuning parameter $\gamma_i > 0$, assuming $\mu_i^T \Omega_i \mu_i$ is small. That is, μ_i is in the span of a set of the eigenvectors corresponding to the smallest eigenvalues of Ω_i . However, selecting the tuning parameters using the user-specified matrices for *QDA* recommended by Molstad and Rothman (2018) becomes computationally cumbersome as one increases the number of classes. Thus, for simplicity we also consider the specified matrices to be $\mathbf{C}_i = \mathbf{0}_p$ and $\mathbf{A}_i = \mathbf{B}_i = \mathbf{I}_p$, which becomes the popular lasso precision matrix shrinkage estimator

$$\hat{\Omega}_i := \arg \min_{\Omega_* \in \mathbb{S}_+^p} \{ \text{tr}(\mathbf{S}_i \Omega_*) - \log |\Omega_*| + \lambda_i^* |\Omega_*|_1 \} \quad (7)$$

proposed by Yuan and Lin (2007). To solve the optimization in (6) and (7), Molstad and Rothman (2018) proposed an alternating direction method-of-multipliers algorithm based on the majorize-minimize principle of Lange (2016).

3.2. Haff Estimator

We next consider the precision matrix shrinkage estimator proposed by Haff (1979a), which induces bias to stabilize the estimator of Ω_i and is given by

$$\hat{\Omega}_i := (1 - t(U_i))(n_i - p - 2)\mathbf{S}_i^{-1} + \frac{t(U_i)(pn_i - p - 2)}{\text{tr}(\mathbf{S}_i)} \mathbf{I}_p, \quad (8)$$

where

$$t(U_i) := \min \left\{ \frac{4(p^2 - 1)}{(n_i - p - 2)p^2}, 1 \right\} U_i^{1/p}$$

and

$$U_i := \frac{p|\mathbf{S}_i|^{1/p}}{\text{tr}(\mathbf{S}_i)}.$$

Here, the ratio U_i quantifies the disparity among the eigenvalues of \mathbf{S}_i , with the numerator and denominator representing the geometric and arithmetic means, respectively. The function $t(U_i)$ serves as the shrinkage factor, controlling the degree of shrinkage applied to \mathbf{S}_i .

3.3. Wang Estimator

The precision matrix estimator proposed by Wang et al. (2015) is the ridge-type shrinkage estimator given by

$$\hat{\boldsymbol{\Omega}}_i := \hat{\alpha}_i(\mathbf{S}_i + \hat{\beta}_i \mathbf{I}_p)^{-1}, \quad (9)$$

where $\hat{\alpha}_i > 0$ and $\hat{\beta}_i > 0$ are shrinkage coefficients under the loss function

$$\frac{1}{p} \text{tr}(\hat{\boldsymbol{\Omega}}_i \boldsymbol{\Sigma}_i - \mathbf{I}_p)^2. \quad (10)$$

This loss function has been utilized by Haff (1979b), Krishnamoorthy and Gupta (1989), and Yang and Berger (1994). We estimate (10) with the empirical loss function

$$L_i(\beta) := 1 - \frac{(\hat{R}_1(\beta))^2}{\hat{R}_2(\beta)}, \quad (11)$$

where

$$\begin{aligned} \hat{R}_1(\beta) &:= \frac{a_1(\beta)}{1 - (p/n_i)a_1(\beta)}, \\ \hat{R}_2(\beta) &:= \frac{a_1(\beta)}{(1 - (p/n_i)a_1(\beta))^3} - \frac{a_2(\beta)}{(1 - (p/n_i)a_1(\beta))^4}, \end{aligned}$$

and $a_1(\beta) := 1 - (1/p)\text{tr}((1/\beta)\mathbf{S}_i + \mathbf{I}_p)^{-1}$ and $a_2(\beta) := (1/p)\text{tr}((1/\beta)\mathbf{S}_i + \mathbf{I}_p)^{-1} - (1/p)\text{tr}((1/\beta)\mathbf{S}_i + \mathbf{I}_p)^{-2}$. By minimizing the empirical loss in (11), we determine that

$$\hat{\beta}_i := \arg \min_{\beta_i \in [\lambda_{\min}, \lambda_{\max}]} L_i(\beta),$$

and

$$\hat{\alpha}_i := \frac{\hat{R}_1(\hat{\beta}_i)}{\hat{R}_2(\hat{\beta}_i)},$$

where λ_{\min} and λ_{\max} are the extrema eigenvalues for \mathbf{S}_i . In the case that $\hat{\beta}_i$ is not unique, we take $\hat{\beta}_i$ to be the smallest solution.

3.4. Bodnar Estimator

Bodnar et al. (2016) have proposed a precision matrix estimator that shrinks toward some user-specified symmetric positive-definite target matrix $\boldsymbol{\Omega}_0$. Let $\|\mathbf{A}\|_F^2 = \text{tr}(\mathbf{A}\mathbf{A}')$ denote the Frobenius norm of a square matrix $\mathbf{A}^{p \times p}$, and let $\|\mathbf{A}\|_{\text{tr}} = \text{tr}(\mathbf{A}\mathbf{A}')^{1/2}$ be the trace norm. Then, for the case where the parameters are unknown, the precision matrix estimator proposed by Bodnar et al. (2016) is

$$\hat{\boldsymbol{\Omega}}_i := \tilde{\alpha}_i \mathbf{S}_i^{-1} + \tilde{\beta} \boldsymbol{\Omega}_0, \text{ for } \sup_p \frac{1}{p} \|\boldsymbol{\Omega}_0\|_{\text{tr}} \leq M, \quad (12)$$

where

$$\tilde{\alpha}_i := 1 - p/n - \frac{(1/n)\|\mathbf{S}_i^{-1}\|_{\text{tr}}^2 \|\boldsymbol{\Omega}_0\|_F^2}{\|\mathbf{S}_i^{-1}\|_F^2 \|\boldsymbol{\Omega}_0\|_F^2 - (\text{tr}(\mathbf{S}_i^{-1} \boldsymbol{\Omega}_0))^2},$$

and

$$\tilde{\beta} := \frac{\text{tr}(\mathbf{S}_i^{-1} \boldsymbol{\Omega}_0)}{\|\boldsymbol{\Omega}_0\|_F^2} (1 - p/n - \tilde{\alpha}_i).$$

For the target matrix, we take $\boldsymbol{\Omega}_0 = \mathbf{I}_p$, which Bodnar et al. (2016) proposed as a naive prior when no information is available concerning $\boldsymbol{\Sigma}_i$. We can utilize information on the precision structure in $\boldsymbol{\Omega}_0$, such as when using $\text{diag}(\mathbf{S}_i)$, to yield sparsity. To ensure the coefficient $\tilde{\beta}_i$ is bounded for large dimensions p , we need only assume that the target matrix $\boldsymbol{\Omega}_0$ is a uniformly-bounded trace norm. That is, an $M > 0$ exists such that $\sup_p (1/p) \|\boldsymbol{\Omega}_0\|_{\text{tr}} \leq M$.

4. A Monte-Carlo Simulation Contrast of Precision Matrix Estimators for SDR

4.1. Monte Carlo Simulation Design

Here, we describe the *MC* simulation design that we used to contrast the classification efficacy of the precision matrix estimators in (6), (8), (9), and (12) in Section 3 in our proposed *SSDR* approach described in Section 2.3. For a baseline, we also considered the sample precision matrix estimator, \mathbf{S}_i^{-1} . We refer to these *SSDR*-based methods as $SSDR_{MRY}$, $SSDR_{Haff}$, $SSDR_{Bod}$, $SSDR_{Wang}$, and $SSDR_{S^{-1}}$. For each *SSDR* method, we use *QDA* as the supervised classifier.

We considered four parameter configurations from multivariate normal populations for our MC simulation study. These are similar to the parameter configurations found in Ounpraseuth et al. (2015) and Wu and Hao (2022) and are given below.

- *Configuration 1*: Different mean vectors with identical spherical covariance matrices and $p = 10$, $\Sigma_1 = \Sigma_2 = \mathbf{I}_p$ and $\mu_1 = \mathbf{0}_p$, $\mu_2 = \mathbf{1}_p$.
- *Configuration 2*: Different covariance matrices consisting of spherical, intra-class, and spiked covariance matrix structures with $p = 10$. $\Sigma_1 = \mathbf{I}_p$, $\Sigma_2 = \Sigma_1 + \mathbf{J}_p$, where \mathbf{J}_p is a $p \times p$ matrix of ones,

$$\Sigma_3 = \begin{bmatrix} 2 & 1 & 0 & 1 & 1 & 1 & 1 & 1 & 1 & 1 \\ 1 & 2 & 0 & 1 & 1 & 1 & 1 & 1 & 1 & 1 \\ 0 & 0 & 10 & 0 & 0 & 0 & 0 & 0 & 0 & 0 \\ 1 & 1 & 0 & 2 & 1 & 1 & 1 & 1 & 1 & 1 \\ 1 & 1 & 0 & 1 & 2 & 1 & 1 & 1 & 1 & 1 \\ 1 & 1 & 0 & 1 & 1 & 2 & 1 & 1 & 1 & 1 \\ 1 & 1 & 0 & 1 & 1 & 1 & 2 & 1 & 1 & 1 \\ 1 & 1 & 0 & 1 & 1 & 1 & 1 & 2 & 1 & 1 \\ 1 & 1 & 0 & 1 & 1 & 1 & 1 & 1 & 2 & 1 \\ 1 & 1 & 0 & 1 & 1 & 1 & 1 & 1 & 1 & 2 \end{bmatrix},$$

and $\mu_1 = (-1.43, -0.66, -0.94, 0.31, -0.19, 0.89, 0.25, -0.34, 1.25, -1.60)'$, $\mu_2 = \mu_1 + \mathbf{1}_p$, and $\mu_3 = \mu_1 + 2\mathbf{1}_p$.

- *Configuration 3*: Two identical covariance matrices with $p = 10$,

$$\Sigma_1 = \Sigma_2 = \begin{bmatrix} 10 & 4 & 5 & 4 & 3 & 4 & 4 & 5 & 4 & 3 \\ 4 & 10 & 5 & 2 & 4 & 3 & 3 & 5 & 4 & 3 \\ 5 & 5 & 10 & 5 & 5 & 3 & 4 & 4 & 4 & 4 \\ 4 & 2 & 5 & 10 & 3 & 4 & 2 & 3 & 4 & 3 \\ 3 & 4 & 5 & 3 & 12 & 3 & 4 & 5 & 3 & 3 \\ 4 & 3 & 3 & 4 & 3 & 9 & 3 & 4 & 4 & 4 \\ 4 & 3 & 4 & 2 & 4 & 3 & 14 & 2 & 2 & 2 \\ 5 & 5 & 4 & 3 & 5 & 4 & 2 & 12 & 1 & -0.5 \\ 4 & 4 & 4 & 4 & 3 & 4 & 2 & 1 & 14 & -1 \\ 3 & 3 & 4 & 3 & 3 & 4 & 2 & -0.5 & -1 & 11 \end{bmatrix},$$

and $\Sigma_3 = \mathbf{I}_p$, with $\mu_1 = \mathbf{0}_p$, $\mu_2 = \mathbf{5}_p$ and $\mu_3 = \mathbf{10}_p$.

- *Configuration 4*: Covariance matrices consisting of spherical and intra-class structures except that $p = 50$. $\Sigma_1 = \mathbf{I}_p$, $\Sigma_2 = \Sigma_1 + 2\mathbf{J}_p$, $\mu_1 = \mathbf{0}_p$, and μ_2 is a $p \times 1$ vector with *IID* entries from the uniform(0, 1) distribution.

In Configurations 2 and 4, for the *SSDR_{MRY}* method, we adopted the user-specified matrices proposed for *QDA* by Molstad and Rothman (2018) given in Section 3.1. For Configurations 1 and 3, the *QDA*-recommended matrices performed the same or worse in terms of the estimated *CER* when contrasted to the simple specified matrices of $\mathbf{C}_i = \mathbf{0}_p$ and $\mathbf{A}_i = \mathbf{B}_i = \mathbf{I}_p$. For Configurations 1 and 3, we used the simple user-specified matrices, which simplified (6) to (7). For the *SSDR_{MRY}* approach, we determined the tuning parameters by minimizing the validation *CERs* across a grid search informed by the eigenvalues of the class-specific sample precision matrices. For each configuration, we generated 5,000 observations from each multivariate normal distribution. We then varied the class-specific training-sample sizes $n_i = p + 1, 2p, 6p, i = 1, \dots, k$, to simulate poorly-posed to well-conditioned covariance matrices. We held the remaining observations per class aside as a test set. For each *SSDR* method, we projected the training and test sets from p to r dimensions and then used *QDA* as the classification rule and recorded the *estimated CER*, denoted \widehat{CER} . We replicated this process 1,000 times for each configuration. For Configuration 4, we generated the parameters once and independently drew all data replicates from the same distribution. Because of the skewness of the distribution of the \widehat{CER} s, we evaluated the classification efficacy in terms of the median of the \widehat{CER} s, denoted as \widehat{CER} . We represented the variability in the \widehat{CER} s by the *standard deviation (SD)*. Also, we used

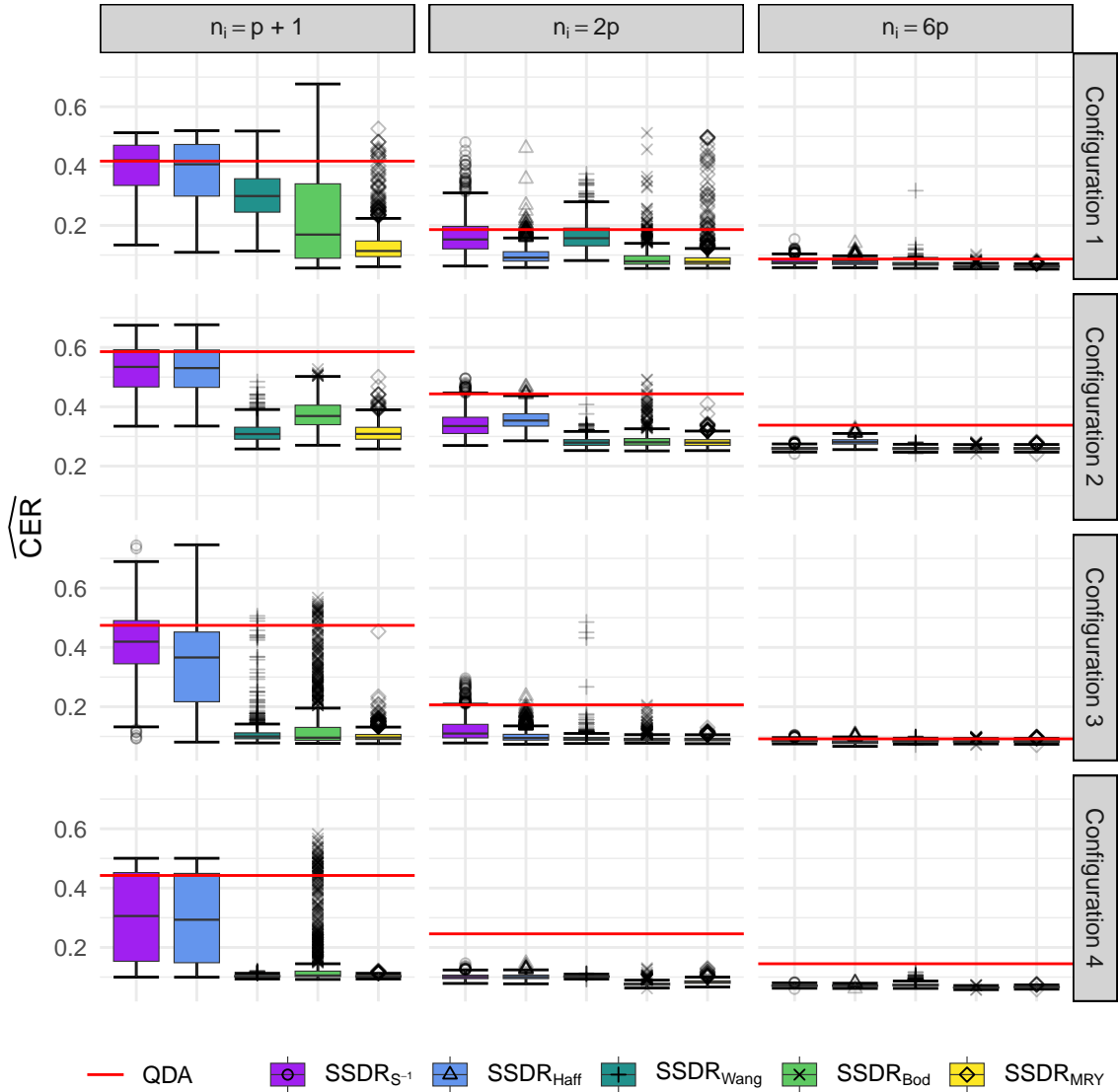


Figure 1: Estimated conditional error rate, denoted \widehat{CER} , plots for the simulation described in Section 4.1 for contrasting the $SSDR$ methods. We display the \widehat{CER} s for the dimension that achieved the global minimum median \widehat{CER} for each method, parameter configuration, and class-specific training-sample size. The full-feature median \widehat{CER} using QDA is represented by the horizontal line.

\widehat{CER}_F to denote the median of the \widehat{CER} s of the full-feature data using only QDA and no dimension reduction. We have summarized our MC simulation results in Figure 1 by displaying the distribution of the \widehat{CER} s for the DRS that achieved the global minimum \widehat{CER} for each class-specific training-sample per parameter configuration. Additionally, the \widehat{CER}_F is given by the horizontal line.

4.2. Monte Carlo Simulation Results

For Configuration 1, we recall that $p = 10$ and the optimal reduced-subspace dimension was $q = 1$. For the full-feature QDA , we determined that the \widehat{CER}_F s for the cases $n_i = p+1$, $2p$, and $6p$ were 0.4167, 0.1858, and 0.0866, respectively. For the case $n_i = p+1 = 11$, the full-data sample covariance matrices were poorly posed because an insufficient number of sample observations were used to inadequately estimate the number of free parameters. Consequently, using the $SSDR_{S^{-1}}$ method resulted in approximately the same \widehat{CER} as \widehat{CER}_F . Moreover, we found that $SSDR_{Haff}$ performed similarly to the $SSDR_{S^{-1}}$ and provided no significant reduction of \widehat{CER}_F . The $SSDR_{Wang}$, $SSDR_{Bod}$, and $SSDR_{MRY}$ methods achieved their respective global minimum \widehat{CER} s of 0.2990 at $r = 6$, 0.1696 at $r = 1$, and 0.1138 at $r = 2$, respectively, per method. Thus, for the given training-sample size, the $SSDR_{MRY}$ method significantly reduced the \widehat{CER}_F by 0.3029.

Although the $SSDR_{Bod}$ notably reduced the \widetilde{CER}_F for this training-sample size, its CER exhibited large variability with a SD of 0.1551. For $n_i = 2p = 20$, only the $SSDR_{Wang}$, $SSDR_{Bod}$, and $SSDR_{MRY}$ yielded notable reductions to the \widetilde{CER}_F with CER s of 0.0914 at $r = 7$, 0.0787 at $r = 1$, and 0.0768 at $r = 1$, respectively. In particular, the $SSDR_{Bod}$ and $SSDR_{MRY}$ methods reduced \widetilde{CER}_F by 0.1000. For the case when $n_i = 6p = 60 > p^2/2$, we usually would not have expected smaller \widetilde{CER} s when contrasted to the \widetilde{CER}_F s for the SDR methods considered here. However, the $SSDR_{Bod}$ and $SSDR_{MRY}$ approaches still reduced the \widetilde{CER}_F by 0.0618 and 0.0615, respectively, for the reduced dimension $r = 1$. In addition, they yielded small SD s of 0.0047 and 0.0037, respectively.

For Configuration 2, we had $p = 10$ and $q = 2$. Using the full-feature QDA , we obtained the \widetilde{CER}_F s corresponding to the class-specific training-sample sizes $n_i = p + 1$, $2p$, and $6p$ of 0.5856, 0.4433, and 0.3379, respectively. For the case where $n_i = p + 1$, the $SSDR_{S-1}$ and $SSDR_{Haff}$ methods showed practically insignificant reductions to \widetilde{CER}_F . However, the $SSDR_{Wang}$, $SSDR_{Bod}$, and $SSDR_{MRY}$ methods resulted in minimum \widetilde{CER} s of 0.3078 at $r = 2$, 0.3688 at $r = 3$, and 0.3083 at $r = 2$, respectively. Thus, for this training-sample size scenario, the $SSDR_{Wang}$ and $SSDR_{MRY}$ methods yielded the largest reduction of \widetilde{CER}_F , approximately 0.2770. Also, the $SSDR_{Wang}$ method had the smallest SD of 0.0311. For the case where $n_i = 2p$, the $SSDR_{Wang}$, $SSDR_{Bod}$, and $SSDR_{MRY}$ methods provided approximately the same \widetilde{CER} of approximately 0.2800 at $r = 2$, resulting in a reduction to \widetilde{CER}_F of approximately 0.1633. Similarly, for the case where $n_i = 6p$, the $SSDR_{S-1}$, $SSDR_{Wang}$, $SSDR_{Bod}$, and $SSDR_{MRY}$ methods yielded approximately the same \widetilde{CER} of about 0.2590, all at $r = 2$, resulting in a reduction to \widetilde{CER}_F of approximately 0.0789. For the two cases when $n_i = 2p$ and $6p$, the $SSDR_{Haff}$ method yielded a slightly increased \widetilde{CER} when contrasted to $SSDR_{S-1}$.

For Configuration 3, $p = q = 10$. For $n_i = p + 1$, $2p$, and $6p$, the \widetilde{CER}_F s were 0.4743, 0.2065, and 0.0917. We remark that although \mathbf{M} was full rank, each of our proposed $SSDR$ -based methods achieved smaller \widetilde{CER} s than \widetilde{CER}_F for all $r < 10$. Specifically, for the case when $n_i = p + 1$, all five $SSDR$ -based methods achieved their minimum \widetilde{CER} at $r = 1$. For this training-sample size, the $SSDR_{Wang}$, $SSDR_{Bod}$, and $SSDR_{MRY}$ methods achieved respective minimum \widetilde{CER} s of 0.0996, 0.0958, and 0.0962. Thus, these three $SSDR$ methods yielded a notable reduction of approximately 0.3700 to \widetilde{CER}_F . However, the $SSDR_{Bod}$ technique resulted in a SD of 0.1017, which was greater than its \widetilde{CER} . In contrast, the SD for the $SSDR_{MRY}$ was 0.0217. Again, we observed that the $SSDR_{S-1}$ and $SSDR_{Haff}$ methods performed similarly to each other with \widetilde{CER} s that yielded little reduction to the \widetilde{CER}_F . For $n_i = 2p$ and $6p$, all $SSDR$ methods yielded similar \widetilde{CER} s between 0.0800 and 0.0900. The two smallest \widetilde{CER} s per training-sample size were 0.0892 by $SSDR_{MRY}$ at $r = 1$ and 0.0804 by $SSDR_{Haff}$ at $r = 4$.

In Configuration 4, we had $p = 50$ and $q = 2$. For $n_i = p + 1$, $2p$, and $6p$, the \widetilde{CER}_F s were 0.4426, 0.2458, and 0.1449, respectively. For $n_i = p + 1 = 51$, the $SSDR_{S-1}$ and $SSDR_{Haff}$ methods yielded similar \widetilde{CER} s of approximately 0.3000, both at $r = 2$. Thus, these \widetilde{CER} s reduced the \widetilde{CER}_F by about 0.1426. However, both of these methods exhibited high variability in CER s with SD s of approximately 0.1443. The $SSDR_{Wang}$ and $SSDR_{MRY}$ methods achieved the same minimum \widetilde{CER} of 0.1030 at $r = 1$, thus yielding a reduction in \widetilde{CER}_F of 0.3396. Moreover, each of these two $SSDR$ approaches yielded small SD s of 0.0041. The $SSDR_{Bod}$ method achieved a similar \widetilde{CER} as the $SSDR_{Wang}$ and $SSDR_{MRY}$ but again exhibited a considerably larger SD of 0.1034. For $n_i = 2p = 100$, all considered $SSDR$ methods notably reduced the \widetilde{CER}_F . The minimum \widetilde{CER} was 0.0706 and was achieved by the $SSDR_{Bod}$ method at $r = 2$ with a SD of 0.0071. For $n_i = 6p = 300 < p^2/2$, unlike in Configurations 1-3, for the $SSDR$ -based \widetilde{CER} , we expected a larger reduction in \widetilde{CER}_F . The global minimum \widetilde{CER} was roughly 0.0700 for the $SSDR_{S-1}$, $SSDR_{Haff}$, and $SSDR_{Wang}$ methods, all with $r = 2$. Moreover, the $SSDR_{Bod}$ and $SSDR_{MRY}$ techniques yielded the two smallest \widetilde{CER} s, both at $r = 2$ of 0.0646 and 0.0665, respectively. Thus, when the data dimensionality was reduced from $p = 50$ to $r = 2$, all five considered $SSDR$ -based approaches significantly reduced \widetilde{CER}_F by approximately 0.0750.

In the MC simulation, the inclusion of the $SSDR_{S-1}$ method demonstrated our proposed $SSDR$ technique's ability to preserve or primarily improve upon the \widetilde{CER}_F in subspaces of dimension $r < p$. More importantly, our MC simulation illustrated a significant improvement in classifier performance achieved through the $SSDR$ approach, which incorporates a user-specified precision shrinkage estimator to stabilize the LDR projection matrix. Across all of the MC simulations, we determined that the $SSDR_{MRY}$ method provided superior or competitive \widetilde{CER} s among the five $SSDR$ methods considered. Moreover, the $SSDR_{MRY}$ method exhibited superior classifier stability, often with the smallest SD , resulting in similar \widetilde{CER} s regardless of the class-specific training-sample size. The $SSDR_{Wang}$ and $SSDR_{Bod}$ methods performed similarly to the $SSDR_{MRY}$ method but yielded slightly larger \widetilde{CER} s for certain parameter and training-sample size scenarios.

Table 1

Datasets used for contrasts that are described in Section 5.1. Class-specific sample sizes, denoted by n_i , are separated by colons.

Dataset	k	n	n_i	p
Autism (AUT)	2	98	36:62	18
Breast Cancer (BRC)	2	683	444:239	9
Divorce (DIV)	2	170	86:84	54
Ionosphere (ION)	2	351	225:126	32
SPECT Heart (SPH)	2	266	211:55	22
Penguins (PNG)	3	333	146:68:119	6
Wheat Seeds (WHS)	3	210	70:70:70	7
Ecoli (ECL)	5	327	143:77:35:20:52	7
Dry Beans (BNS)	7	13,611	2027:1322:522:1630:1928:2636:3546	16

5. Real Data Applications

5.1. Data and Analysis Description

Here, we considered nine real datasets from the University of California - Irvine (UCI) Machine Learning Repository. These are listed in Table 1. The number of populations ranged from 2 to 7 classes, the total sample sizes varied from 98 to 13,611, and the number of original features ranged from 6 to 54. More information on the datasets is given in Appendix A. We remark that, when it was needed, we “studentized” the data or added random error from the $N(0, \sigma = 10^{-5})$ distribution to features causing covariance matrix singularity issues.

We used the nine real datasets given in Table 1 to contrast the classification efficacy of the same five *SSDR* methods considered in the *MC* simulation in Section 4. Again, we reduced the data dimension using each *SSDR* method and then applied the *QDA* classifier. For each dataset and *SSDR* method, we performed repeated 10-fold cross-validation in which we took the mean value of the \widehat{CER} s for the 10 folds, denoted as \overline{CER} , and then repeated this process 1,000 times. The classification performance was evaluated in terms of the median value of the \widehat{CER} s, \overline{CER} , and we also calculated the *SD* of the \widehat{CER} s. We then reported the \widehat{CER}_F s, the \widehat{CER} s for the reduced dimension, r^* , that achieved the global minimum \overline{CER} for each *SSDR* method, and the corresponding *SDs* in Table 2.

For the Breast Cancer, Divorce, Ionosphere, and Penguins datasets, we used the user-specified matrices proposed by Molstad and Rothman (2018) for *QDA* in the *SSDR_{MRY}* method. Additionally, because of different magnitudes among the features, we determined that standardizing the mean vectors in the recommended *QDA*-specified matrices improved classification performance for the Breast Cancer, Ionosphere, and Penguins datasets. For the remaining datasets, we used the simple user-specified matrices for the *SSDR_{MRY}* technique.

5.2. Real Data Contrasts of Precision Matrix Estimators for SDR

In Table 2, for the Autism, Breast Cancer, Ionosphere, and Penguins datasets, we see that we obtained \overline{CER} reductions for the chosen subspaces when they were contrasted to the full feature-dimensional \widehat{CER}_F , regardless of the particular *SSDR* method used. In the table, we display only the global minimum \overline{CER} corresponding to the selected reduced dimensions $r^* < p$. However, when $r = p$ held, our *SSDR* method still preserved or improved on the \widehat{CER}_F for all datasets, regardless of the precision matrix estimator used.

Notably, across all datasets considered here, the *SSDR_{MRY}* technique consistently outperformed its five competitors by yielding the smallest \widehat{CER} s, thus providing the largest reduction to the corresponding \widehat{CER}_F s. For example, for the Autism dataset, the *SSDR_{MRY}* method achieved a $\widehat{CER} = 0.0111$ compared to the $\widehat{CER}_F = 0.1400$. Thus, for this dataset, the *SSDR_{MRY}* method significantly reduced the \widehat{CER}_F by 0.1289, while reducing the dimensionality from $p = 18$ to $r = 2$. Additionally, for the Penguins dataset, the *SSDR_{MRY}* method yielded an impressive $\widehat{CER} = 0.00$. This result provided a reduction of 0.0810 to the \widehat{CER}_F . Moreover, the *SSDR_{MRY}* method exhibited superior classifier stability for *QDA* with the smallest *SD* for seven of the nine datasets. We attribute the excellent performance of the *SSDR_{MRY}* approach to the induced sparsity of the *MRY* estimator. In fact, we determined that the percentage of zero entries in the averaged *MRY* precision matrix estimators from our repeated cross-validation simulation was 31%, compared to approximately 5% for the other precision shrinkage estimators considered here.

The *SSDR_{Haff}* method generally exhibited subpar performance, often yielding approximately the same or slightly larger \widehat{CER} s than *SSDR_{S-1}*. Although second to *SSDR_{MRY}*, the *SSDR_{Wang}* method consistently showed significant reductions in \widehat{CER} s across all datasets. Additionally, the *SSDR_{Wang}* approach also had smaller \widehat{CER} s when contrasted to the *SSDR_{S-1}* method and the \widehat{CER}_F . Additionally, for the Divorce dataset, *SSDR_{Wang}* achieved the same global minimum

Table 2

Median estimated conditional error rates, denoted \widetilde{CER} , for real data classification applications described in Section 5.1 for contrasting $SSDR$ methods coupled with QDA . The global minimum \widetilde{CER} % is given followed by the (SD) and then the reduced-dimension size that achieves the minimum \widetilde{CER} %, [r^*]. The full dimensional \widetilde{CER}_F % using the QDA is denoted by QDA . Smallest observed \widetilde{CER} s are typeset in bold per dataset.

Dataset	QDA	$SSDR_{S^{-1}}$	$SSDR_{Haf}$	$SSDR_{Wang}$	$SSDR_{Bod}$	$SSDR_{MRY}$
AUT	14.0 (2.02)	10.1 (1.77) [6]	11.4 (1.77) [5]	6.75 (1.31) [5]	5.02 (1.35) [4]	1.11 (0.75) [2]
BCR	4.97 (0.15)	3.80 (0.19) [2]	4.10 (0.14) [3]	3.80 (0.14) [2]	3.80 (0.19) [2]	3.80 (0.14) [2]
DIV	13.5 (0.61)	13.6 (0.48) [2]	13.6 (0.48) [2]	1.11 (0.47) [3]	1.18 (0.21) [1]	1.11 (0.47) [3]
ION	12.5 (0.49)	5.99 (0.71) [8]	5.99 (0.71) [8]	6.24 (0.53) [8]	6.27 (0.70) [8]	5.19 (0.43) [9]
SPH	21.7 (1.03)	20.0 (0.85) [21]	19.9 (0.82) [18]	16.6 (0.93) [2]	16.5 (0.80) [1]	15.8 (0.56) [1]
PNG	8.10 (0.52)	17.3 (0.98) [5]	17.3 (0.98) [5]	0.60 (0.36) [5]	0.29 (0.24) [4]	0.00 (0.19) [5]
WHS	5.24 (0.41)	6.19 (0.65) [6]	6.19 (0.65) [6]	3.81 (0.45) [6]	6.19 (0.67) [6]	2.86 (0.49) [5]
ECL	23.1 (0.96)	26.0 (1.07) [6]	25.4 (1.23) [6]	17.2 (1.05) [5]	18.9 (0.87) [6]	11.3 (0.56) [4]
BNS	8.85 (0.04)	8.99 (0.04) [15]	8.99 (0.04) [15]	8.60 (0.04) [7]	8.99 (0.04) [15]	8.29 (0.04) [5]

\widetilde{CER} of 0.0111 as $SSDR_{MRY}$. The $SSDR_{Bod}$ \widetilde{CER} s notably improved the \widetilde{CER}_F s for all datasets except the Dry Beans and Wheat Seeds datasets. However, the $SSDR_{Bod}$ method was always inferior to the $SSDR_{MRY}$ approach.

5.3. Real Data Contrasts of Current SDR and Supervised Classification Methods

In both the MC simulation and real data applications considered in Sections 4 and 5.2, we determined that the $SSDR_{MRY}$ method produced a well-conditioned projection matrix due to the prominent sparsity in the MRY precision matrix estimator. Here, using the same nine real datasets as in Section 5.2, we contrasted the performance of our newly-proposed $SSDR_{MRY}$ method with four current SDR and supervised classification methods. These techniques consist of a sparse linear discriminant method ($MSDA$) from Mai et al. (2019), an updated version of SIR that uses lasso regression ($SIRL$) proposed by Lin et al. (2019), the envelope discriminant subspace method ($ENDS$) of Zhang and Mai (2019), and a one-dimensional SDR method that is based on the optimal one-dimensional QDA error rate ($QDAP$) from Wu and Hao (2022). We remark that the approach derived by Wu and Hao (2022) was applicable for only two populations.

To compare the performance of each method, we performed the repeated 10-fold cross-validation procedure described in Section 5.1 to obtain estimates for the CER . For fair comparison, we used QDA as the classifier for each SDR -based method. We have graphically displayed the CER s for each method in Figure 2. When applicable, to minimize the corresponding \widetilde{CER} s, we determined all reduced dimensions and tuning parameters via cross-validation for each method.

The proposed $SSDR_{MRY}$ method outperformed the competing $ENDS$, $SIRL$, $QDAP$, and $MSDA$ methods by achieving the smallest \widetilde{CER} for six of the nine datasets. These six datasets were the Autism, Divorce, Ionosphere, SPECT Heart, Penguins, and Dry Beans datasets. Additionally, our $SSDR_{MRY}$ technique was the only method that consistently improved upon the \widetilde{CER}_F for every dataset. For example, for the Ionosphere dataset, with the exception of our $SSDR_{MRY}$ method, all the SDR and classification methods yielded \widetilde{CER} s greater than the $\widetilde{CER}_F = 0.1250$. However, for the Ionosphere dataset, our proposed $SSDR_{MRY}$ method reduced the data dimension from $p = 32$ to $r = 8$ and achieved a $\widetilde{CER} = 0.0519$. Thus, $SSDR_{MRY}$ reduced the \widetilde{CER}_F by 0.0731. Once again, we attribute the $SSDR_{MRY}$ method's efficacy to its preservation of differences in the classes and the improved stability of its projection matrix, which prevents over-parameterizing regardless of the training-sample sizes.

The $ENDS$ method achieved the minimum $\widetilde{CER} = 0.0279$ for the Breast Cancer dataset; however, this \widetilde{CER} was within a standard error of the CER s of the $QDAP$ and $SIRL$ methods. The $SIRL$ method yielded competitive CER s. However, the method never achieved the smallest CER for any of the nine datasets. Moreover, the $SIRL$ method yielded a CER greater than the \widetilde{CER}_F for the Dry Beans and Ionosphere datasets. We note that the $ENDS$ and $SIRL$ methods often achieved their minimum CER in the same or smaller subspace dimension as the $SSDR_{MRY}$ method. However, we believe that their bias towards smaller reduced dimensions led to a lack of robustness for datasets with a large original feature-space, often resulting in larger \widetilde{CER} s because of a reduced data representation that was too small to preserve all important original discrimination information. The $QDAP$ performance was similar to that of the considered competitive methods, except for the SPECT Heart dataset, where it yielded a significantly larger $\widetilde{CER} = 0.5678$ when contrasted to the $\widetilde{CER}_F = 0.2170$. The $MSDA$ method achieved the minimum CER s of 0.0238 and 0.1106 for the Wheat Seeds and Ecoli datasets, respectively. However, for these two datasets, the $SSDR_{MRY}$ method gave \widetilde{CER} s of 0.0286 and 0.1127, which were only slightly greater than the $MSDA$ CER s. Additionally, similar to the $SIRL$ method, for the Dry Beans dataset, the $MSDA$ method had a larger \widetilde{CER} of 0.0979 when contrasted to the $\widetilde{CER}_F = 0.0885$.

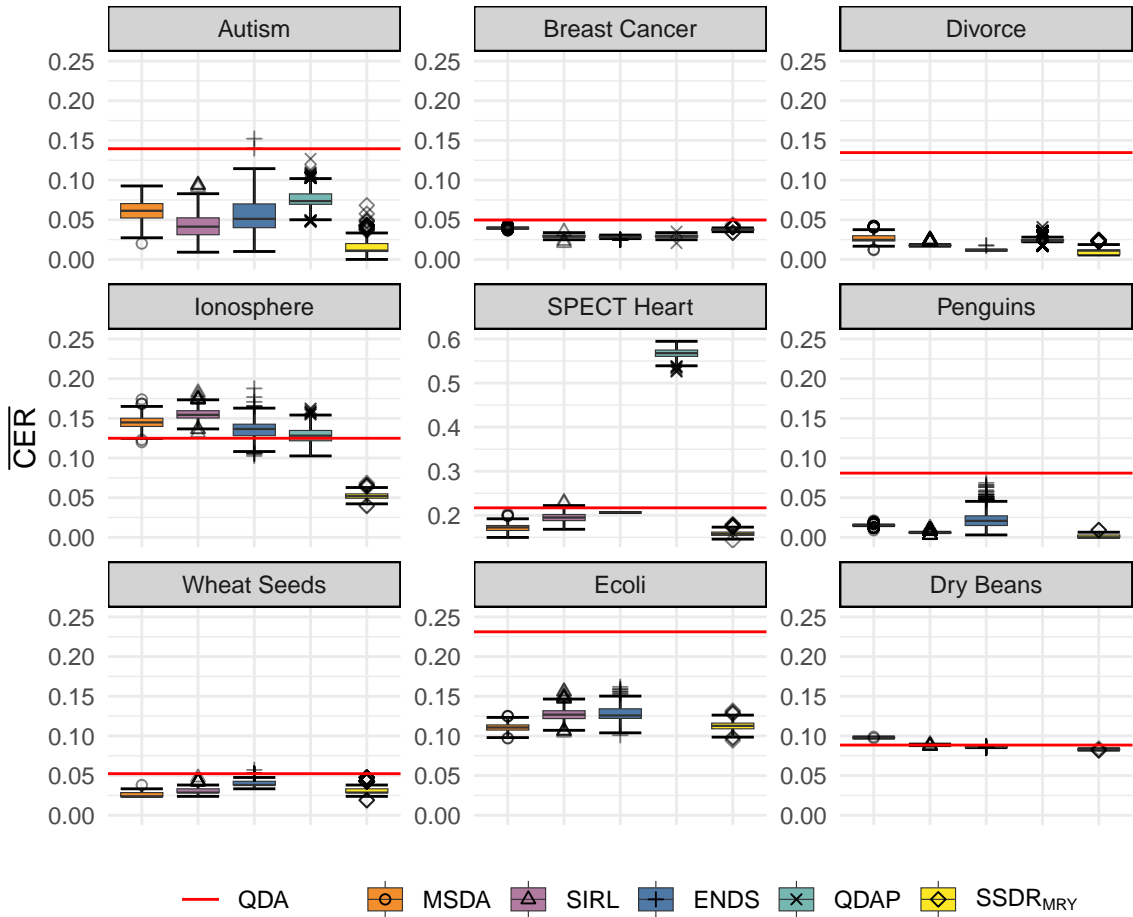


Figure 2: Mean 10-fold cross-validation *conditional error rate*, denoted \overline{CER} , plots for comparison of *MSDA*, *SIRL*, *ENDS*, *QDAP*, and *SSDR_{MRY}* methods as described in Section 5.3. The full-dimensional median \overline{CER} using *QDA* is given by the horizontal line. The *QDAP* method is applicable only to binary response data and is not displayed for some datasets. The y-axis scale is from 0.00 to 0.25 for all datasets except the *SPECT Heart* dataset.

6. Discussion

In this paper, we derived a theoretical *SDR* method that preserves the optimal error rate under the *QDA* decision rule in a reduced dimension, $q < p$. Additionally, when parameter estimation is required, we have proposed a new *SDR* technique, *stabilized SDR* (*SSDR*), which utilizes a user-specified precision matrix shrinkage estimator to improve stability of the projection matrix. This proposed *SSDR* method is particularly useful, though not limited to, training-sample-size scenarios where $p < n_i < p^2/2$. We have examined multiple precision matrix estimators to use in our proposed *SSDR* method. Through *MC* simulations and real data applications, we have determined that the *SSDR_{MRY}* method improved the dimension reduction subspace for supervised classification, often preserving class differences more effectively than the other precision matrix estimators considered here. Additionally, the *SSDR_{MRY}* method induces sparsity, which reduces the number of parameters to be estimated and significantly decreases the variability of the *QDA* classifier.

Through empirical studies, we have demonstrated that our *SSDR_{MRY}* method often achieved superior classification efficacy by producing smaller estimated *CERs*, thus frequently outperforming several current competitive *SDR* and supervised classification methods. Although we do not claim that *SSDR_{MRY}* always yields the smallest estimated *CER*, we have found considerable evidence that when training-sample sizes are small relative to the original feature-space dimension, the *SSDR_{MRY}* method in conjunction with the *QDA* decision rule offers a highly competitive *SDR* and classification method for heteroscedastic populations. In summary, we have developed a new *SDR* method that provides improved projection matrix stability and, therefore, *QDA* classifier stability. We have promoted *SDR*-enhancing properties through induced sparsity and improved precision matrix estimation by employing a user-specified precision matrix shrinkage estimator.

6.1. Code Availability

We performed the MC simulations and real data applications using the statistical programming language R, version 4.3.1. We implemented R package `HDSHP` for the *Bodnar* estimator and the R package `SCPME` for the *MRY* precision matrix estimator. In addition, we programmed the *Haff* and *Wang* precision matrix estimators because they were not readily available in R. We implemented the *MSDA* and *SIRL* approaches in the R packages `TULIP` and `LassoSIR`, respectively, and also formatted the *ENDS* method in MATLAB using the code provided by the original authors in their supplementary material. Additionally, we configured the *QDAP* method using the R package available on the authors' github site. Our new *SSDR* method is implemented in the working `sdr` package available at <https://github.com/D3r1kBoonstra/sdr>. Lastly, one can find all reproducible code for the simulations and graphical figures at https://github.com/D3r1kBoonstra/Stabilized_SDR.

Acknowledgements

The authors of this research article received no grant money from funding agencies in the public, commercial, or not-for-profit sectors. We also thank Mrs. Joy Young for her grammar recommendations that enhanced the quality of our writing.

Appendix A. Additional Dataset Information

Here, we give additional information on the datasets used in Section 5.3. The Autism data from Thabtah (2017) pertains to autistic spectrum disorder screening for adolescents. The Wisconsin Breast Cancer Diagnostic data is from Street et al. (1993) and contains data to classify breast tissue as benign or malignant using features from images of a fine needle aspirate of the breast tissue. The Divorce data, introduced by Yöntem et al. (2019), consists of an ordinal questionnaire, referred to as the Divorce Predictor Scale. The Ionosphere data originates from Sigillito et al. (1989) and classifies electrons as "good" or "bad" using features from a signal collection system. The SPECT Heart data from Kurgan et al. (2001) covers abnormalities in cardiac single-proton emission-computed tomography. Palmer's Penguins data from Gorman et al. (2014) is likened to the Iris data in Fisher (1936) for teaching machine learning and uses various measurements of penguins to classify them into particular species. The Wheat Seed data, provided by Charytanowicz et al. (2010), consists of geometric parameters from X-ray images of three wheat kernel species. The Ecoli data from Horton and Nakai (1996) refers to the cellular location sites of protein. We removed classes `omL`, `imL`, and `imS` because of sample covariance matrix singularity due to insufficient class-specific training-sample sizes. Lastly, extracted features from high-resolution camera images were used to create the Dry Beans data in Koklu and Ozkan (2020).

Appendix B. Proofs of Three Lemmas

Lemma 1. Let $\mathbf{W} \in \mathbb{R}^{p \times s}$, where $s := (k-1)(p+1)$, be

$$\mathbf{W} := [\mathbf{g}_2 - \mathbf{g}_1 | \dots | \mathbf{g}_k - \mathbf{g}_1 | \mathbf{H}_2 - \mathbf{H}_1 | \dots | \mathbf{H}_k - \mathbf{H}_1],$$

where $\mathbf{g}_i \in \mathbb{R}^p$, $\mathbf{H}_i \in \mathbb{S}^p$, and $\mathbf{g}_1 \neq \mathbf{g}_j$ and $\mathbf{H}_1 \neq \mathbf{H}_j$ for at least one value of k , where $2 \leq j \leq k$ and $i = 1, \dots, k$. Also, let $\text{rank}(\mathbf{W}) = 1 \leq q < p$, and let $\mathbf{U} \in \mathbb{R}^{p \times q}$, $\mathbf{U}^T \mathbf{U} = \mathbf{I}_q$, $\mathbf{D} \in \mathbb{R}^{q \times q}$, and $\mathbf{V} \in \mathbb{R}^{s \times q}$ be the matrix components of the reduced SVD of \mathbf{W} such that $\mathbf{W} = \mathbf{UDV}^T$ with $\text{rank}(\mathbf{U}) = q$, and let $\mathbf{P}_\mathbf{U} := \mathbf{UU}^T$. Then,

- (a) $\mathbf{P}_\mathbf{U}(\mathbf{g}_i - \mathbf{g}_1) = \mathbf{g}_i - \mathbf{g}_1$; $\mathbf{P}_\mathbf{U}(\mathbf{H}_i - \mathbf{H}_1) = \mathbf{H}_i - \mathbf{H}_1$,
- (b) $\mathbf{P}_\mathbf{U}^\perp(\mathbf{g}_i - \mathbf{g}_1) = \mathbf{0}$; $\mathbf{P}_\mathbf{U}^\perp(\mathbf{H}_i - \mathbf{H}_1) = \mathbf{0}$,
- (c) $\mathbf{P}_\mathbf{U}(\mathbf{H}_i - \mathbf{H}_1) = (\mathbf{H}_i - \mathbf{H}_1)\mathbf{P}_\mathbf{U}$,
- (d) $\mathbf{P}_\mathbf{U}\mathbf{H}_i = \mathbf{H}_i\mathbf{P}_\mathbf{U}$,
- (e) $\mathbf{P}_\mathbf{U}^\perp\mathbf{H}_i = \mathbf{H}_i\mathbf{P}_\mathbf{U}^\perp$.

Proof. For parts (a) and (b), note that $\mathbf{g}_i - \mathbf{g}_1, \mathbf{H}_i - \mathbf{H}_1 \in \mathcal{C}(\mathbf{U})$, and $\mathbf{g}_i - \mathbf{g}_1, \mathbf{H}_i - \mathbf{H}_1 \in \mathcal{N}(\mathbf{P}_\mathbf{U}^\perp)$, where $i \in \{2, \dots, k\}$. For part (c), because $\mathbf{H}_i \in \mathbb{S}^p$, we have

$$\mathbf{P}_\mathbf{U}[\mathbf{H}_i - \mathbf{H}_1] = [\mathbf{H}_i - \mathbf{H}_1]^T = [\mathbf{H}_i - \mathbf{H}_1]\mathbf{P}_\mathbf{U}.$$

For part (d), recall that for $\mathbf{x} \in \mathbb{R}^{p \times 1}$, $\mathbf{x}^T \mathbf{P}_\mathbf{U}$ projects \mathbf{x} onto the row space of $\mathbf{P}_\mathbf{U}$. Because $\mathbf{P}_\mathbf{U} \in \mathbb{S}_p$, the column space and row space are equal. Thus, $\mathbf{P}_\mathbf{U}\mathbf{H}_i = \mathbf{H}_i\mathbf{P}_\mathbf{U}$. Finally, for (e), we have by parts (b) and (d) that

$$\begin{aligned} \mathbf{P}_\mathbf{U}^\perp(\mathbf{H}_i - \mathbf{H}_1) = \mathbf{0} &\iff \mathbf{P}_\mathbf{U}^\perp\mathbf{H}_i = \mathbf{H}_1 - \mathbf{P}_\mathbf{U}\mathbf{H}_1 \\ &\iff \mathbf{P}_\mathbf{U}^\perp\mathbf{H}_i = \mathbf{H}_1 - \mathbf{H}_1\mathbf{P}_\mathbf{U} \\ &\iff \mathbf{P}_\mathbf{U}^\perp\mathbf{H}_i = \mathbf{H}_1\mathbf{P}_\mathbf{U}^\perp. \end{aligned}$$

□

Lemma 2. Consider the matrices \mathbf{U} , $\mathbf{P}_\mathbf{U}$, and \mathbf{H}_i , $i = 1, \dots, k$, defined in Lemma 1. Then, $[\mathbf{U}^T \mathbf{H}_i \mathbf{U}]^{-1} = \mathbf{U}^T \mathbf{H}_i^{-1} \mathbf{U}$.

Proof. Using Lemma 1(d), we have that

$$\begin{aligned} (\mathbf{U}^T \mathbf{H}_i \mathbf{U})(\mathbf{U}^T \mathbf{H}_i^{-1} \mathbf{U}) &= \mathbf{U}^T \mathbf{H}_i \mathbf{P}_\mathbf{U} \mathbf{H}_i^{-1} \mathbf{U} \\ &= \mathbf{U}^T \mathbf{P}_\mathbf{U} \mathbf{H}_i \mathbf{H}_i^{-1} \mathbf{U} \\ &= \mathbf{U}^T \mathbf{U} \\ &= \mathbf{I}. \end{aligned}$$

□

Lemma 3. Consider \mathbf{U} , \mathbf{g}_i , and \mathbf{H}_i , $i = 1, \dots, k$, defined in Lemma 1. Also, let $\mathbf{C} = \mathbf{R} [\mathbf{I} - \mathbf{U} \mathbf{U}^T] \in \mathbb{R}^{(p-q) \times p}$, where $\mathbf{R} \in \mathbb{R}^{(p-q) \times p}$ such that $\text{rank}(\mathbf{C}) = p - q$. Then, we have that

- (a) $\mathbf{C} \mathbf{g}_i = \mathbf{C} \mathbf{g}_1$,
- (b) $\mathbf{C} \mathbf{H}_i \mathbf{C}^T = \mathbf{C} \mathbf{H}_1 \mathbf{C}^T$.

Proof. The proof of (a) follows trivially from Lemma 1(b). Also, by Lemma 1(d), note that

$$\begin{aligned} \mathbf{U}^T \mathbf{H}_i \mathbf{C}^T &= \mathbf{U}^T \mathbf{H}_i (\mathbf{I}_p - \mathbf{U} \mathbf{U}^T)^T \mathbf{R}^T \\ &= (\mathbf{U}^T \mathbf{H}_i - \mathbf{U}^T \mathbf{H}_i \mathbf{U} \mathbf{U}^T) \mathbf{R}^T \\ &= \mathbf{0}. \end{aligned}$$

Then by Lemma 1 (b), $\mathbf{C} \mathbf{H}_i \mathbf{C}^T - \mathbf{C} \mathbf{H}_i \mathbf{U} (\mathbf{U}^T \mathbf{H}_i \mathbf{U})^{-1} \mathbf{U}^T \mathbf{H}_i \mathbf{C}^T = \mathbf{C} \mathbf{H}_1 \mathbf{C}^T$. □

References

Anderson, T.W., 1951. Classification by multivariate analysis. *Psychometrika* 16, 31–50. doi:10.1007/BF02313425.

Bellman, R.E., 1961. Adaptive Control Processes. Princeton University Press, Princeton. doi:10.1515/9781400874668.

Bodnar, T., Gupta, A.K., Parolya, N., 2016. Direct shrinkage estimation of large dimensional precision matrix. *Journal of Multivariate Analysis* 146, 223–236. doi:10.1016/j.jmva.2015.09.010. special Issue on Statistical Models and Methods for High or Infinite Dimensional Spaces.

Charytanowicz, M., Niewczas, J., Kulczycki, P., Kowalski, P.A., Łukasik, S., Źak, S., 2010. Complete gradient clustering algorithm for features analysis of x-ray images, in: *Information Technologies in Biomedicine: Volume 2*, Springer. pp. 15–24. doi:10.1007/978-3-642-13105-9_2.

Cook, R.D., 1998. Regression Graphics: Ideas for Studying Regressions Through Graphics. Wiley Series in Probability and Statistics, Wiley. doi:10.1002/9780470316931.

Cook, R.D., 2018. Principal components, sufficient dimension reduction, and envelopes. *Annual Review of Statistics and Its Application* 5, 533–559. doi:10.1146/annurev-statistics-031017-100257.

Cook, R.D., Weisberg, S., 1991. Sliced inverse regression for dimension reduction: Comment. *Journal of the American Statistical Association* 86, 328–332. doi:10.2307/2290564.

Cook, R.D., Zhang, X., 2014. Fused estimators of the central subspace in sufficient dimension reduction. *Journal of the American Statistical Association* 109, 815–827. doi:10.1080/01621459.2013.866563.

Eckart, C., Young, G., 1936. The approximation of one matrix by another of lower rank. *Psychometrika* 1, 211–218. doi:10.1007/BF02288367.

Fan, J., Liao, Y., Liu, H., 2016. An overview of the estimation of large covariance and precision matrices. *The Econometrics Journal* 19, C1–C32. doi:10.1111/ectj.12061.

Fisher, R.A., 1936. The use of multiple measurements in taxonomic problems. *Annals of Eugenics* 7, 179–188. doi:10.1111/j.1469-1809.1936.tb02137.x.

Gaynanova, I., Booth, J.G., Wells, M.T., 2016. Simultaneous sparse estimation of canonical vectors in the $p >> n$ setting. *Journal of the American Statistical Association* 111, 696–706. doi:10.1080/01621459.2015.1034318.

Gorman, K.B., Williams, T.D., Fraser, W.R., 2014. Ecological sexual dimorphism and environmental variability within a community of antarctic penguins (genus *pygoscelis*). *PLoS one* 9, e90081. doi:10.1371/journal.pone.0090081.

Haff, L.R., 1979a. Estimation of the inverse covariance matrix: Random mixtures of the inverse Wishart matrix and the identity. *The Annals of Statistics* 7, 1264–1276. doi:10.1214/aos/1176344845.

Haff, L.R., 1979b. An identity for the Wishart distribution with applications. *Journal of Multivariate Analysis* 9, 531–544. doi:10.1016/0047-259X(79)90056-3.

Horton, P., Nakai, K., 1996. A probabilistic classification system for predicting the cellular localization sites of proteins., in: Ismb, St. Louis, Missouri, USA. pp. 109–115. URL: <https://www.ncbi.nlm.nih.gov/pubmed/8877510>.

Koklu, M., Ozkan, I.A., 2020. Multiclass classification of dry beans using computer vision and machine learning techniques. *Computers and Electronics in Agriculture* 174, 105507. doi:10.1016/j.compag.2020.105507.

Krishnamoorthy, K., Gupta, A.K., 1989. Improved minimax estimation of a normal precision matrix. *The Canadian Journal of Statistics / La Revue Canadienne de Statistique* 17, 91–102. doi:10.2307/3314766.

Kurgan, L.A., Cios, K.J., Tadeusiewicz, R., Ogiela, M., Goodenday, L.S., 2001. Knowledge discovery approach to automated cardiac spect diagnosis. *Artificial Intelligence in Medicine* 23, 149–169. doi:10.1016/s0933-3657(01)00082-3.

Lange, K., 2016. MM optimization algorithms. Society for Industrial and Applied Mathematics, Philadelphia, PA. doi:10.1137/1.9781611974409.

Li, B., 2018. Sufficient Dimension Reduction: Methods and Applications with R. Chapman & Hall/CRC Monographs on Statistics and Applied Probability, CRC Press. doi:10.1201/9781315119427.

Li, K.C., 1991. Sliced inverse regression for dimension reduction. *Journal of the American Statistical Association* 86, 316–327. doi:10.1080/01621459.1991.10475035.

Lin, Q., Zhao, Z., Liu, J.S., 2019. Sparse sliced inverse regression via lasso. *Journal of the American Statistical Association* 114, 1726–1739. doi:10.1080/01621459.2018.1520115.

Mai, Q., Shao, X., Wang, R., Zhang, X., 2025. Slicing-free inverse regression in high-dimensional sufficient dimension reduction. *Statistica Sinica* doi:10.5705/ss.202022.0112.

Mai, Q., Yang, Y., Zou, H., 2019. Multiclass sparse discriminant analysis. *Statistica Sinica* 29, 97–111. doi:10.5705/ss.202016.0117.

Molstad, A.J., Rothman, A.J., 2018. Shrinking characteristics of precision matrix estimators. *Biometrika* 105, 563–574. doi:10.1093/biomet/asy023.

Ounpraseuth, S., Young, P., Van Zyl, J., Nelson, T., Young, D., 2015. Linear dimension reduction for multiple heteroscedastic multivariate normal populations. *Open Journal of Statistics* 05, 311–333. doi:10.4236/ojs.2015.54033.

Peters, B.C., Redner, R., Decell, H.P., 1978. Characterizations of linear sufficient statistics. *Sankhyā: The Indian Journal of Statistics, Series A* 40, 303–309.

Qian, W., Ding, S., Cook, R.D., 2019. Sparse minimum discrepancy approach to sufficient dimension reduction with simultaneous variable selection in ultrahigh dimension. *Journal of the American Statistical Association* 114, 1277–1290. doi:10.1080/01621459.2018.1497498.

Sigillito, V.G., Wing, S.P., Hutton, L.V., Baker, K.B., 1989. Classification of radar returns from the ionosphere using neural networks. *Johns Hopkins APL Technical Digest* 10, 262–266.

Street, W.N., Wolberg, W.H., Mangasarian, O.L., 1993. Nuclear feature extraction for breast tumor diagnosis, in: *Biomedical Image Processing and Biomedical Visualization, SPIE*. pp. 861 – 870. doi:10.1117/12.148698.

Thabtah, F., 2017. Autism spectrum disorder screening: Machine learning adaptation and dsm-5 fulfillment, in: *Proceedings of the 1st International Conference on Medical and Health Informatics 2017*, Association for Computing Machinery. p. 1–6. doi:10.1145/3107514.3107515.

Wang, C., Pan, G., Tong, T., Zhu, L., 2015. Shrinkage estimation of large dimensional precision matrix using random matrix theory. *Statistica Sinica* 25, 993–1008. doi:10.5705/ss.2012.328.

Wu, R., Hao, N., 2022. Quadratic discriminant analysis by projection. *Journal of Multivariate Analysis* 190, 104987. doi:10.1016/j.jmva.2022.104987.

Xie, J., Qiu, Z., 2007. The effect of imbalanced data sets on lda: A theoretical and empirical analysis. *Pattern Recognition* 40, 557–562. doi:10.1016/j.patcog.2006.01.009.

Xue, J.H., Titterington, D.M., 2008. Do unbalanced data have a negative effect on lda? *Pattern Recognition* 41, 1558–1571. doi:10.1016/j.patcog.2007.11.008.

Yang, R., Berger, J.O., 1994. Estimation of a Covariance Matrix Using the Reference Prior. *The Annals of Statistics* 22, 1195 – 1211. doi:10.1214/aos/1176325625.

Yuan, M., Lin, Y., 2007. Model selection and estimation in the gaussian graphical model. *Biometrika* 94, 19–35. doi:10.1093/biomet/asm018.

Yöntem, M.K., Adem, K., İlhan, T., Kılıçarslan, S., 2019. Divorce prediction using correlation based feature selection and artificial neural networks. *Nevşehir Hacı Bektaş Veli Üniversitesi SBE Dergisi* 9, 259–273.

Zeng, J., Mai, Q., Zhang, X., 2024. Subspace estimation with automatic dimension and variable selection in sufficient dimension reduction. *Journal of the American Statistical Association* 119, 343–355. doi:10.1080/01621459.2022.2118601.

Zhang, X., Mai, Q., 2019. Efficient integration of sufficient dimension reduction and prediction in discriminant analysis. *Technometrics* 61, 259–272. doi:10.1080/00401706.2018.1512901.